bioRxiv preprint doi: https://doi.org/10.1101/132092; this version posted April 28, 2017. The copyright holder for this preprint (which was not certified by peer review) is the author/funder. All rights reserved. No reuse allowed without permission.

N-(3-oxododecanoyl)-L-homoserine lactone interactions in the breast tumor microenvironment: implications for breast cancer viability and proliferation *in vitro*

Brittany N. Balhouse[1,2], Logan Patterson[3,4], Eva M. Schmelz[5], Daniel J. Slade[3], Scott S. Verbridge[1,2,*]

[1] School of Biomedical Engineering and Sciences, Virginia Tech-Wake Forest University, Blacksburg, VA, United States of America

[2] Department of Biomedical Engineering and Mechanics, Virginia Tech, Blacksburg, VA, United States of America

[3] Department of Biochemistry, Virginia Tech, Blacksburg, VA, United States of America

[4]Department of Pathology, University of Virginia, Charlottesville, VA, United States of America

[5]Department of Human Nutrition, Foods and Exercise, Virginia Tech, Blacksburg, VA, United States of America

* Corresponding author

Email: sverb@vt.edu

bioRxiv preprint doi: https://doi.org/10.1101/132092; this version posted April 28, 2017. The copyright holder for this preprint (which was not certified by peer review) is the author/funder. All rights reserved. No reuse allowed without permission.

Abstract It is well documented that the tumor microenvironment profoundly impacts the etiology and progression of cancer, and the contribution of the resident microbiome within breast tissue remains poorly understood. Tumor microenvironmental conditions such as hypoxia and dense tumor stroma predispose progressive phenotypes and therapy resistance, yet the role of bacteria in this interplay remains uncharacterized. We hypothesized that the effect of individual bacterial secreted molecules on breast cancer viability and proliferation would be modulated by these tumor-relevant stressors differentially for cells at varying stages of progression. To test this, we incubated human breast adenocarcinoma cells (MDA-MB-231, MCF-DCIS.com) and non-malignant breast epithelial cells (MCF-10A) with N-(3-oxododecanoyl)-L-homoserine lactone (OdDHL), a quorum-sensing molecule from *Pseudomonas aeruginosa* that regulates bacterial stress responses. *Pseudomonas* was recently characterized as a significant fraction of the breast tissue microbiome and OdDHL is documented to have significant effects on mammalian cells. We found differences in the MDA-MB-231 and MCF-DCIS.com viability after OdDHL treatment that were cell type and culture condition (i.e. microenvironment) dependent. This result was in contrast to the MCF-10A cells, which demonstrated no change in viability over the OdDHL concentration range examined, in any culture condition. We further determined that the observed trends in breast cancer viability were due to modulation of proliferation for both cell types, as well as the induction of necrosis for MDA-MB-231 cells in all conditions. Our results provide evidence that bacterial quorum-sensing molecules interact with the host environment to modulate breast cancer viability and proliferation, and that the effect of OdDHL is dependent on both cell type as well as microenvironment. Understanding the interactions between bacterial signaling molecules and the host tissue environment will allow for

bioRxiv preprint doi: https://doi.org/10.1101/132092; this version posted April 28, 2017. The copyright holder for this preprint (which was not certified by peer review) is the author/funder. All rights reserved. No reuse allowed without permission.

47 future studies that determine the contribution of bacteria to the onset, progression, and therapy
48 response of breast cancer.
49
50 **Introduction** The tumor microenvironment is now a widely recognized and well-studied
51 contributor to cancer dynamics, particularly for breast cancer. While increased matrix density,
52 programming of cancer-associated stromal cells, evolving gradients of oxygen and nutrients, and
53 leaky vasculature have all been implicated as key players in breast cancer progression (1-4), the
54 impact of the recently identified breast tissue resident microbiotic niche has received little
55 attention. Beyond the effects of pathogenic or tumorigenic bacteria such as *Chlamydophila*
56 *pneumonia*, *Salmonella typhi*, *Streptococcus gallolyticus* (5), *Helicobacter pylori (6)* and
57 *Fusobacterium nucleatum* (7), the majority of analyses of tumor-microbiome interactions have
58 centered on local cell-cell interactions within the gut microenvironment, or more systemic
59 immune effects influenced by gut microbiota (8). Only a handful of studies have been conducted
60 to investigate the influences of tissue-resident bacteria in other tumor sites, such as for breast
61 cancer (9-11). Even fewer have investigated how small molecules released from resident bacteria
62 may interact with cells in the presence of other critical microenvironmental factors, e.g. tumor
63 hypoxia, to regulate cancer progression. In an effort to address these questions, we investigated
64 interactions between the quorum-sensing molecule N-(3-oxododecanoyl)-L-homoserine lactone
65 (OdDHL) and the breast tumor relevant microenvironmental cues of a stiff collagen-derived
66 tissue mimic and hypoxia. This representative study will aid in our understanding of how the
67 understudied breast tissue microbiome may contribute to disease phenotypes, patient-to-patient
68 variability, and cancer progression.
69

bioRxiv preprint doi: https://doi.org/10.1101/132092; this version posted April 28, 2017. The copyright holder for this preprint (which was not certified by peer review) is the author/funder. All rights reserved. No reuse allowed without permission.

OdDHL secreting *Pseudomonas* are Gram-negative Proteobacteria that were recently found to make up a significant fraction of the microbiome within breast tissue (12), and on nipple skin and aspirate from women with and without a history of breast cancer (13). In addition, *Pseudomonas* has been shown to make up a significant portion of the bacteria found in human breast milk (11, 14-16). *Pseudomonas* was among the top five most abundant genera for both sample populations in the 2014 study by Urbaniak et al. (12) and in several studies of breast milk microbiota (14). OdDHL is a quorum-sensing molecule associated with biofilm development and environmental stress response in bacteria (17) that has been shown to promote apoptosis in a variety of human cell lines (18-23). Especially interesting is its selective effect inhibiting proliferation and inducing apoptosis in breast cancer cells, but not in non-malignant breast cells (21). For these reasons, studying the effects of OdDHL is not only important from the basic science perspective (e.g. regarding its role in the tumor microenvironment), but also from the therapeutic perspective given its potential as an anti-cancer treatment (24, 25).

High tissue density is not only a risk factor for breast cancer development, but also a clinical diagnostic tool (26). Increased stroma density (resulting from increased collagen deposition and cross-linking in the extracellular matrix (ECM)) is also associated with phenotypic changes in both cancer cells and normal stroma cells (27). In an *in vitro* setting, growing cells on or within a collagen hydrogel, as opposed to on a polystyrene substrate in two-dimensions (2D), changes not only the type of focal adhesions cells make with their environment (28), but also how cells respond to stresses within that environment (e.g. chemotherapeutic agents) (27, 29, 30). Three-dimensional (3D) cellular adhesions are implicated in reduced cellular response to chemotherapeutics (a phenomenon called adhesion-mediated resistance) and a progressive

bioRxiv preprint doi: https://doi.org/10.1101/132092; this version posted April 28, 2017. The copyright holder for this preprint (which was not certified by peer review) is the author/funder. All rights reserved. No reuse allowed without permission.

phenotype (27, 31, 32). Hypoxia is also a well-documented constituent of the solid tumor microenvironment; angiogenesis cannot keep up with the rate of tumor growth and produces a gradient of oxygen from the well-fed periphery to a necrotic core that is devoid of oxygen (33). Similar to cancer cells in a 3D environment, a low oxygen environment is associated with a progressive phenotype and a resistance to chemotherapy (33, 34). Although, adhesion- and hypoxia-mediated resistance have been extensively demonstrated for chemotherapeutic compounds, adhesion- and hypoxia-mediated regulation of cellular response to bacterial signaling molecules has not yet been investigated. Despite the previous research into OdDHL, the role of OdDHL in the context of breast tumor microenvironmental stressors was still unknown. Because such stressors are associated with altered cell responses (e.g. chemoresistance), it was our hypothesis that OdDHL would differentially modulate breast cancer cell viability and proliferation in hypoxia and in 3D culture (in which cells are seeded in the bulk of a tissue mimic).

In an effort to make a preliminary characterization of the response for both metastatic and non-metastatic subtypes of breast cancer, we utilized MDA-MB-231 and MCF-DCIS.com cells, respectively. MCF-10A breast epithelial cells were used as a non-malignant control. Both MDA-MB-231 and MCF-10A cells were chosen for this research because of their wide documentation in the literature (35, 36). The MCF-DCIS.com cell line, which is derived from the MCF-10A line (37, 38), offers an intermediary model cell between the MCF-10A and MDA-MB-231 lines; not only does it represent a pre-invasive, non-metastatic form of breast cancer, but is Her2+ (37) whereas the MDA-MB-231 line is triple negative (35). In addition, both necrotic cores and desmoplasia have been observed in lesions from MCF-DCIS.com injections (38) as well as in

bioRxiv preprint doi: https://doi.org/10.1101/132092; this version posted April 28, 2017. The copyright holder for this preprint (which was not certified by peer review) is the author/funder. All rights reserved. No reuse allowed without permission.

MDA-MB-231 xenografts (39, 40), motivating our studies in hypoxia- and adhesion-mediated resistance.

Methods

Cell culture. We used MDA-MB-231 triple negative breast cancer cells (ATCC® HTB-26™), MCF-DCIS.com ductal carcinoma *in situ* breast cancer cells (generously donated by Dr. Eva M. Schmelz) (38), and MCF-10A breast epithelial cells (ATCC® CRL-10317™) for our malignant versus non-malignant cell comparison. MDA-MB-231 cells were cultured in DMEM/F12 (1:1) media supplemented with 10% fetal bovine serum and 1% penicillin-streptomycin (PS). MCF-10A and MCF-DCIS.com cells were cultured in DMEM/F12 (1:1) media supplemented with 5% horse serum, 1% PS, 0.05% hydrocortisone, 0.1% human insulin, 0.02% epidermal growth factor, and 0.01% cholera toxin. Hereafter, these supplemented DMEM/F12 (1:1) media will be referred to as complete media. Cells were subcultured every 4-5 days and used until passage 50. Stock cells were grown in T-75 flasks under standard culture conditions (37°C incubator with 5% CO_2, and ambient O_2 (referred to hereafter as normoxia).

For 2D experimental conditions, cells were seeded in 48-well polystyrene plates at a concentration of 100,000 cells per milliliter (30,000 cells per well), with two plates seeded per cell type per experiment. After seeding, all plates were incubated under standard culture conditions in normoxia. After 24 hours, the media was changed in all wells and the plates that were to undergo the hypoxia treatment were moved into an incubator with 1% oxygen and the standard culture conditions of 37°C, 5% CO_2.

bioRxiv preprint doi: https://doi.org/10.1101/132092; this version posted April 28, 2017. The copyright holder for this preprint (which was not certified by peer review) is the author/funder. All rights reserved. No reuse allowed without permission.

3D culture. 3D culture was defined as cells suspended throughout a tissue mimic, namely a rat tail derived type I collagen hydrogel. The collagen stock was manufactured using a technique described previously (41). Briefly, collagen was extracted from Sprague-Dawley rat tails (Bioreclamation, Inc), sterilized in 70% ethanol, and dissolved in 0.1% glacial acetic acid for three days. The dissolved collagen stock was then aliquoted, frozen, lyophilized, and stored at –20°C. At least three days prior to use, the lyophilized collagen was reconstituted in 0.1% glacial acetic acid at a concentration of 12 milligrams of collagen per milliliter of acetic acid solution, and this dissolved stock solution was then used for up to four weeks post re-constitution.

The hydrogel was created by neutralizing the collagen stock with empirically derived proportions of 10X DMEM, 1X DMEM/F12 (1:1) and 1M sodium hydroxide (NaOH) (revised from (41)) to create a hydrogel with pH 7.4 and 6 mg/mL of collagen in 0.1% acetic acid solution. During the neutralization process, all solutions were kept on ice to prevent collagen polymerization. Cells were suspended throughout the hydrogel by resuspension of a cell pellet into the required 1X DMEM/F12 (1:1) prior to its addition into the unpolymerized (but neutralized) hydrogel solution. Cells were seeded in the hydrogel solution at a concentration of three million cells per milliliter of solution (~300,000 cells per well). The hydrogel solution was pipetted into pretreated SYLGARD® 184 silicone elastomer molds topped with untreated coverslips to create approximately 1 mm thick discs comprised of ~0.1 mL hydrogel solution. The hydrogels were incubated for 30 minutes at 37°C, then transferred into 24-well plates and covered with 0.6 mL complete media standard of the included cell type. There was one plate of 3D samples per cell type. All 3D samples were maintained in an incubator under standard culture conditions (37°C,

bioRxiv preprint doi: https://doi.org/10.1101/132092; this version posted April 28, 2017. The copyright holder for this preprint (which was not certified by peer review) is the author/funder. All rights reserved. No reuse allowed without permission.

161 5% CO_2, normoxia). Hydrogels with no cells were also created as a control for the alamarBlue™
162 cell viability assay described below.
163
164 *OdDHL treatment.* Two days after seeding, the appropriate complete media containing varying
165 concentrations of OdDHL were added to the samples. The concentrations of OdDHL reflect
166 levels documented in the literature as physiological values in a niche in close proximity to the
167 bacteria producing the quorum sensing molecule (42). For the OdDHL stock solution,
168 lyophilized OdDHL (Sigma-Aldrich) was reconstituted in dimethyl sulfoxide (DMSO) at a
169 concentration of 67.25 mM or 20 mg/mL (the maximum solubility of OdDHL in DMSO). For
170 the experimental solutions, the OdDHL stock solution was added to the complete medium
171 appropriate for the cell line (as described above) to create the highest concentration (400 µM)
172 OdDHL solution. Serial 1:2 dilutions of the stock solution were performed in DMSO to create
173 200 µM, 100 µM, 50 µM, and 25 µM solutions in complete medium. A control of 0.6% DMSO
174 (the volume per volume percentage of DMSO in all OdDHL treatments) was used. Cells were
175 treated with the OdDHL or control solutions for 24 hours before proliferation (by EdU assay)
176 and apoptosis/necrosis (by annexin V and propidium iodide assay) was analyzed, and 48 hours
177 before viability (by alamarBlue™ assay) was analyzed. The difference in incubation period was
178 determined by the nature of the assay to be performed.
179
180 *alamarBlue™ cell health assay.* After the OdDHL or control treatment, the treatment solutions
181 were removed and fresh complete medium supplemented with 10% alamarBlue™ solution
182 (Thermo Fisher Scientific) was added to all wells, including 2D and 3D negative control wells
183 where there were no cells. These were incubated in normoxic or hypoxic incubators until

bioRxiv preprint doi: https://doi.org/10.1101/132092; this version posted April 28, 2017. The copyright holder for this preprint (which was not certified by peer review) is the author/funder. All rights reserved. No reuse allowed without permission.

positive control wells (0.6% DMSO control) were magenta in color; reduction rate was dependent on cell type and culture condition. When controls wells showed the color change, three subsamples were taken from the solution of each well and added to a 96-well plate. As per the manufacturer's instructions, the 96-well plates were read on a spectrophotometer, which analyzed the absorbance at 570 and 600 nm wavelengths. The percent reduction of alamarBlue™ was calculated with the equation recommended by the manufacturer, namely:

$$Percent\ Reduction\ of\ alamarBlue^{TM} = \left(\frac{(O_2 \times A_1) - (O_1 \times A_2)}{(R_1 \times N_2) - (R_2 \times N_1)}\right) \times 100$$

where O_1 is the molar extinction coefficient (E) of oxidized alamarBlue™ at 570 nm, O_2 is the E of oxidized alamarBlue™ at 600 nm, R_1 is the E of reduced alamarBlue™ at 570 nm, R_2 is the E of reduced alamarBlue™ at 570 nm, A_1 is the absorbance of the test well at 570 nm, A_2 is the absorbance of the test well at 600 nm, N_1 is the absorbance of the negative control at 570 nm and N_2 is the absorbance of the negative control at 600 nm. The average percent reduction of alamarBlue™ for each experimental group was divided by the average percent reduction of the 0 µM OdDHL (0.6% DMSO) control to calculate a relative viability.

EdU assay. An EdU assay was performed to study the effect of OdDHL on proliferation of cells in normoxia (2D), hypoxia (2D), and 3D (normoxia). The EdU assay was conducted using the Click-iT® EdU Alexa Fluor 488® Imaging Kit (Thermo Fisher Scientific) as per the manufacturer's instructions, with the exception of the fixing where 10% formalin was substituted for 3.7% formaldehyde. Briefly, after incubation with OdDHL in the various experimental conditions for 24 hours, half of the experimental solution was removed and fresh complete medium supplemented with the EdU molecule was added to each well (including controls). After a two hour incubation, the samples were fixed with 10% formalin (15 minutes for 2D, 45

bioRxiv preprint doi: https://doi.org/10.1101/132092; this version posted April 28, 2017. The copyright holder for this preprint (which was not certified by peer review) is the author/funder. All rights reserved. No reuse allowed without permission.

minutes for 3D), washed and incubated with the Click-iT® reaction cocktail to fluorescently label cells that entered the S-phase of the cell cycle during the two hour incubation period. Cells were then counterstained with DAPI. Wells were imaged under 100X magnification with 1 subsample per well for 2D conditions and, using a confocal microscope, 5 subsamples per well for 3D conditions vertically through the hydrogel volume (30 µm spacing). The images were post-processed in ImageJ; see Supporting Information for more information on post-processing (Fig S1). The area of cell nuclei stained with Alexa Fluor 488® was divided by the area of cell nuclei stained with DAPI to find the fraction of cells entering S-phase during the 2 hour incubation period.

Apoptosis/necrosis assay. The apoptosis and necrosis response was determined by incubation with annexin V-FITC (AV-FITC) and propidium iodide (PI) using a commercial assay (Annexin V-FITC Apoptosis Kit, BioVision Inc.). The assay was completed according to manufacturer instructions for all 2D samples and with three times the recommended incubation time for 3D samples. After incubation, cells were immediately imaged using 100X magnification with 3 subsamples per well for 2D conditions and, using a confocal microscope, 5 subsamples per well for 3D conditions vertically through the hydrogel volume (30 µm spacing). The images were post-processed in ImageJ; see Supporting Information for more information on post-processing (Fig S2). All values are relative to the appropriate 0.6% DMSO control for each experimental condition.

bioRxiv preprint doi: https://doi.org/10.1101/132092; this version posted April 28, 2017. The copyright holder for this preprint (which was not certified by peer review) is the author/funder. All rights reserved. No reuse allowed without permission.

Statistical analysis. For each experiment, there were two wells per experimental condition and control and each experiment was conducted three times (N = 3), unless otherwise noted. The statistics are based on the average values for each condition in each experiment.

The statistical analyses consisted of a full factorial two-way analysis of variance (ANOVA) in which the differences in viability (relative percent reduction of alamarBlue™), proliferation rate (percent of cells entering S-phase), and apoptosis/necrosis (AV-FITC/PI stained cells) for varying culture conditions and OdDHL concentrations were analyzed for each cell line tested. Where a p-value < 0.05 was found for the ANOVA, post-hoc Tukey tests and least means contrasts were performed to analyze the degree of significance between experimental conditions. Error bars represent standard error of the mean.

Results It was found that the response to OdDHL was dependent not only on cell-type, but also the culture condition. As compared to the control, the malignant MDA-MB-231 cells showed significantly different responses to 400 µM of OdDHL in all culture conditions (Fig 1A-1E). In the 2D/normoxia condition, the 400 µM OdDHL treatment corresponded to approximately 52.2% (± 2.2%) viability, relative to the control. In the 2D/hypoxia condition, that relative viability was increased to 60.6% (± 2.2%) and in 3D/normoxia condition, that viability was increased to 81.9% (± 2.2%) (Fig 1C and Fig 1D, respectively). There were significant decreases in the MDA-MB-231 viability at the 100 and 200 µM levels of OdDHL, as compared to the control, for the 2D conditions as well (Fig 1A and Fig 1B). In contrast, the non-malignant MCF-10A cells exposed to OdDHL showed no significant change in viability relative to the control across all concentrations in all culture conditions (Fig 1F-1H).

bioRxiv preprint doi: https://doi.org/10.1101/132092; this version posted April 28, 2017. The copyright holder for this preprint (which was not certified by peer review) is the author/funder. All rights reserved. No reuse allowed without permission.

Figure 1. **OdDHL has a cell-specific and significant impact on MDA-MB-231 viability in all culture conditions**.

Significant differences in mean MDA-MB-231 viability at 100, 200 and 400 µM concentrations relative to the control in hypoxia and normoxia in 2D (A) and 3D and 2D in normoxia (B); *** = p-value < 0.0001, ** = p-value < 0.01, * = p-value < 0.05 based on Tukey post-hoc differences. Significant differences in MDA-MB-231 viability relative to the control between culture conditions with 400 µM treatment in hypoxia and normoxia in 2D (C) and 3D and 2D in normoxia (D); *** = p-value < 0.0001, ** = p-value < 0.01 based on least mean contrasts. (E) Photomicrographs of MDA-MB-231 cells cultured in normoxia (2D), hypoxia (2D), and 3D (normoxia) with fluorescence microscopy (with DAPI staining; scale bar = 100 µm) at 100X magnification after 24 hours of OdDHL treatment. (F) Photomicrographs of MCF-10A cells cultured in normoxia (2D), hypoxia (2D), and 3D (normoxia) with fluorescence microscopy (with DAPI staining; scale bar = 100 µm) at 100X magnification after 24 hours of OdDHL treatment. Differences in MCF-10A viability relative to the control at 100, 200 and 400 µM concentrations in hypoxia and normoxia in 2D (G) and 3D and 2D in normoxia (H).

The viability assay of the MCF-DCIS.com cells showed the cells responded in a similar fashion to MDA-MB-231 cells in both the 2D/normoxia and 2D/hypoxia conditions, with significant dose-dependent decreases in viability with increasing OdDHL concentrations (Fig 2A). However, unlike the MDA-MB-231 cells, the MCF-DCIS.com cells did not have a significant decrease in viability in the 3D/normoxia condition at any treatment level of OdDHL (Fig 2B). Also, unique to the MCF-DCIS.com cells is a significantly lower viability at the 400 µM level

bioRxiv preprint doi: https://doi.org/10.1101/132092; this version posted April 28, 2017. The copyright holder for this preprint (which was not certified by peer review) is the author/funder. All rights reserved. No reuse allowed without permission.

for MCF-DCIS.com cells cultured in 2D/hypoxia than those cultured in 2D/normoxia (Fig 2C). However, for MCF-DCIS.com cells grown in 3D versus 2D in normoxia, there was significantly increased MCF-DCIS.com viability with the 400 μM OdDHL treatment (Fig 2D). An analysis of the cell specific viability response to 400 μM OdDHL showed that MCF-DCIS.com cells have significantly higher viability than MDA-MB-231 cells, but significantly lower viability than MCF-10A cells when cultured under the 2D/normoxia condition (Fig 2E). With the same treatment, MCF-DCIS.com cells showed significantly lower viability than MCF-10A cells when cultured under the 2D/hypoxia (a response that is statistically not different from that of MDA-MB-231 cells under the same condition) (Fig 2E). When cells were cultured under the 3D/normoxia condition, there was no difference in MCF-DCIS.com viability as compared to MCF-10A cell viability with the 400 μM OdDHL treatment; both were significantly higher than MDA-MB-231 cell viability under the same condition (Fig 2F).

Figure 2. **OdDHL has a cell-specific and differential impact on MCF-DCIS.com cells dependent on culture condition**.

Significant differences in mean MCF-DCIS.com viability relative to the control at 100, 200 and 400 μM OdDHL concentrations in hypoxia and normoxia in 2D (A) and 3D and 2D in normoxia (B); *** = p-value < 0.0001, ** = p-value < 0.01, * = p-value < 0.05 based on Tukey post-hoc differences. Significant differences in MCF-DCIS.com viability relative to the control between culture conditions with 400 μM OdDHL treatment in hypoxia and normoxia in 2D (C) and 3D and 2D in normoxia (D); *** = p-value < 0.0001 based on least mean contrasts. Significant differences in mean MCF-10A, MCF-DCIS.com, MDA-MB-231 viabilities relative to the

bioRxiv preprint doi: https://doi.org/10.1101/132092; this version posted April 28, 2017. The copyright holder for this preprint (which was not certified by peer review) is the author/funder. All rights reserved. No reuse allowed without permission.

control at 400 µM OdDHL concentrations in hypoxia and normoxia in 2D (E) and 3D and 2D in normoxia (F); *** = p-value < 0.0001 based on Tukey post-hoc differences.

The results of the proliferation assay paralleled the results of the viability assay for both the MDA-MB-231 and MCF-DCIS.com cells. The percentage of cells entering the S-phase of the cell cycle during the two-hour incubation period with EdU was significantly lower for 400 µM OdDHL-treated MDA-MB-231 cells than for control (0.6% DMSO) cells across all culture conditions (Fig 3A, Fig 3B). The comparison of MDA-MB-231 proliferation between the different culture conditions can more readily be seen in Fig 3C and Fig 3D. The percentage of EdU-tagged cells after the two hour incubation period was also lower for 400 µM OdDHL-treated versus the control cells across all culture conditions for the MCF-DCIS.com cells. The comparison of MCF-DCIS.com proliferation between the different culture conditions can more readily be seen in Fig 3G and Fig 3H.

Figure 3. 400 µM OdDHL treatment significantly impacts the proliferation rate of MDA-MB-231 and MCF-DCIS.com cells in all conditions.
Significant differences in the mean percent of MDA-MB-231 cells entering S-phase of proliferation in the 0.6% DMSO and 400 µM OdDHL treatment groups in hypoxia and normoxia in 2D for N = 4 (A) and 3D and 2D in normoxia for N = 3 (B); *** = p-value < 0.0001 based on least mean contrasts. The relative percent of MDA-MB-231 cells entering S-phase with the 400 µM OdDHL treatment for cells in hypoxia versus normoxia in 2D (C) and cells in 3D versus 2D in normoxia (D). Significant differences in the mean percent of MCF-DCIS.com cells entering S-phase of proliferation in the 0.6% DMSO and 400 µM OdDHL treatment groups in hypoxia and

bioRxiv preprint doi: https://doi.org/10.1101/132092; this version posted April 28, 2017. The copyright holder for this preprint (which was not certified by peer review) is the author/funder. All rights reserved. No reuse allowed without permission.

normoxia in 2D for N = 4 (A) and 3D and 2D in normoxia for N = 3 (B); ** = p-value < 0.001, * = p-value < 0.05 based on least mean contrasts. The relative percent of MCF-DCIS.com cells entering S-phase with the 400 μM OdDHL treatment for cells in hypoxia versus normoxia in 2D (G) and cells in 3D versus 2D in normoxia (H).

The apoptosis/necrosis assay revealed that OdDHL also induces cell death. Analysis of the mean gray value (MGV) for the AV-FITC staining showed that apoptosis of MDA-MB-231 cells with 400 μM OdDHL relative to the 0.6% DMSO control in all culture conditions was not significantly increased (Fig 4A). Analysis of the MGV for the PI staining showed significantly increased necrosis of MDA-MB-231 with 400 μM OdDHL treatment, relative to the 0.6% DMSO control, in all culture conditions (Fig 4B). Analysis of MGV for the AV-FITC and PI staining of MCF-DCIS.com cells showed significantly increased apoptosis and necrosis, respectively, only for cells in 2D/normoxia with the 400 μM OdDHL treatment (Fig 4C and Fig 4D). The PI staining of the MCF-DCIS.com cells in the 3D/normoxia showed that these cells had decreased necrosis with 400 μM OdDHL treatment, relative to the control (Fig 4D). The 400 μM OdDHL did not significantly increase apoptosis or necrosis of MCF-10A cells compared to the 0.6% DMSO control (Fig 4E and Fig 4F). Rather, 400 μM OdDHL significantly decreased both MCF-10A apoptosis and necrosis under the 3D/normoxia condition compared to the 0.6% DMSO control (Fig 4E and Fig 4F).

Figure 4. 400 μM OdDHL treatment significantly increases necrosis of MDA-MB-231 cells in all conditions.

bioRxiv preprint doi: https://doi.org/10.1101/132092; this version posted April 28, 2017. The copyright holder for this preprint (which was not certified by peer review) is the author/funder. All rights reserved. No reuse allowed without permission.

(A) Differences in the annexin V-FITC staining mean gray value (MGV) for MDA-MB-231 cells treated with 400 μM OdDHL, normalized to 0.6% DMSO control for 3D/normoxia, 2D/hypoxia, and 2D/normoxia culture conditions (N = 3). (B) Differences in the propidium iodide staining MGV for MDA-MB-231 cells treated with 400 μM OdDHL, normalized to 0.6% DMSO control for 3D/normoxia, 2D/hypoxia, and 2D/normoxia culture conditions (N = 3); ** = p-value < 0.01, * = p-value < 0.05 based on least mean contrasts. (C) Differences in the annexin V-FITC staining MGV for MCF-DCIS.com cells treated with 400 μM OdDHL, normalized to 0.6% DMSO control for 3D/normoxia (N = 3), 2D/hypoxia (N = 4), and 2D/normoxia culture conditions (N = 4); *** = p-value < 0.001 based on least mean contrasts. (D) Differences in the propidium iodide staining MGV for MCF-DCIS.com cells treated with 400 μM OdDHL, normalized to 0.6% DMSO control for 3D/normoxia, 2D/hypoxia, and 2D/normoxia culture conditions (N = 3); ** = p-value < 0.01, * = p-value < 0.05 based on least mean contrasts. (E) Differences in the annexin V-FITC staining MGV for MCF-10A cells treated with 400 μM OdDHL, normalized to 0.6% DMSO control for 3D/normoxia, 2D/hypoxia, and 2D/normoxia culture conditions (N = 3); ** = p-value < 0.01 based on least mean contrasts. (F) Differences in the propidium iodide staining MGV for MCF-10A cells treated with 400 μM OdDHL, normalized to 0.6% DMSO control for 3D/normoxia, 2D/hypoxia, and 2D/normoxia culture conditions (N = 3); ** = p-value < 0.01 based on least mean contrasts.

Discussion The analysis of the viability of MDA-MB-231and MCF-10A cells in response to OdDHL confirmed our hypotheses that there would be reduced MDA-MB-231 response to OdDHL treatment in both hypoxia and in 3D while MCF-10A cells would show no such changes. As we anticipated, cells cultured in a 3D environment had the highest relative viability

bioRxiv preprint doi: https://doi.org/10.1101/132092; this version posted April 28, 2017. The copyright holder for this preprint (which was not certified by peer review) is the author/funder. All rights reserved. No reuse allowed without permission.

(Fig 1) with OdDHL treatment as compared to cells in 2D. Cells in hypoxia also had increased relative viability with OdDHL treatment as compared to those in normoxia (Fig 1). Thus, we found that OdDHL preferentially affects MDA-MB-231 cells as compared to MCF-10A cells and this effect is blunted by both hypoxia and 3D culture.

It is interesting to note that, while MDA-MB-231 cells had a decreased viability response when cultured under hypoxia and 3D conditions, the MCF-DCIS.com cells did not respond in the same way (Fig 2). MCF-DCIS.com viability was in-between that of the MCF-10A and MDA-MB-231 cells in 2D/normoxia, statistically similar to the MDA-MB-231 response in 2D/hypoxia, and statistically similar to the MCF-10A response in 3D/normoxia (Fig 2). This novel evidence suggests that bacterial factors may affect mammalian cells differently at each stage of cancer progression. It is possible that the response to OdDHL is linked to epithelial-to-mesenchymal transition as it has previously been shown that OdDHL has an effect on cytoskeletal proteins in multiple malignant cell lines (24, 43). OdDHL may be differentially affecting the MDA-MB-231 cells in comparison to the MCF-DCIS.com cells due to its mesenchymal and highly metastatic characteristics; however, much more work needs to be done for confirmation of this hypothesis.

In order to better understand the decreases in viability for the breast cancer cells as measured by the alamarBlue™ assay, we decided to examine the effect of OdDHL on both cell proliferation and apoptosis/necrosis. For MDA-MB-231 cells, it was revealed that OdDHL has two mechanisms to decrease the cell number. We found that OdDHL significantly decreases proliferation of MDA-MB-231 cells in all culture conditions (Fig 3). We then hypothesized that decrease in proliferation alone could not account for the decrease in viability we observed. A

bioRxiv preprint doi: https://doi.org/10.1101/132092; this version posted April 28, 2017. The copyright holder for this preprint (which was not certified by peer review) is the author/funder. All rights reserved. No reuse allowed without permission.

386 second mechanism of action was found in the apoptosis/necrosis assay. We found that necrosis
387 of MDA-MB-231 cells was significantly increased with the 400 μM OdDHL treatment as
388 compared to the 0.6% DMSO control (Fig 4).
389
390 This effect was not seen in MCF-10A cells and, in fact, was reversed for MCF-10A cells
391 cultured in the 3D/normoxia condition (Fig 4). The fact that OdDHL triggers necrosis as opposed
392 to apoptosis is not surprising; bacteria are known to induce necrosis (44). However, the fact that
393 OdDHL may reduce apoptosis and necrosis for non-malignant cells under a stressful
394 microenvironment (i.e. a stiff collagen matrix) is intriguing. More research is needed to
395 understand the selectivity of necrosis induction and, especially, reduction by OdDHL.
396
397 Likewise, we found that the primary mechanism responsible for the decrease in MCF-DCIS.com
398 cell number seen with OdDHL treatment was decreased proliferation (Fig 3). The decreased
399 proliferation was observed in all three culture conditions, which seemed to conflict with the lack
400 of decreased viability seen for MCF-DCIS.com cells in the 3D/normoxia condition. The
401 apoptosis/necrosis assay shed some light on this seemingly contradictory result. It was found
402 that, as with the MCF-10A cells, there was decreased necrosis for MCF-DCIS.com cells in the
403 3D/normoxia condition (Fig 4). From these data, it seems that the opposing effects of the
404 decreased proliferation and the decreased necrosis caused by the 400 μM OdDHL treatment
405 countered each other, leading to the invariable response in viability observed. Like the MDA-
406 MB-231 cells, the MCF-DCIS.com cells in the 2D/normoxia condition also exhibited increased
407 necrosis; however, these cells also had increased apoptosis (Fig 4). Taken together, these data are
408 indicative that there may be different mechanisms of OdDHL action on cancer viability and these

bioRxiv preprint doi: https://doi.org/10.1101/132092; this version posted April 28, 2017. The copyright holder for this preprint (which was not certified by peer review) is the author/funder. All rights reserved. No reuse allowed without permission.

409 are cell type and microenvironmental condition dependent. While more work with cells
410 representative of varying stages of progression needs to be completed, these preliminary data
411 suggest that OdDHL may be more effective at suppressing the growth of more malignant or
412 advanced breast cancer.
413
414 Future studies investigating the possible role of tumor microenvironmental microbiota should
415 establish if, as is suggested here, OdDHL suppresses highly malignant phenotypes. In addition,
416 further experiments should extend the study of non-malignant and pre-malignant cell types to
417 establish if, as seems to be the case for MCF-10A cells, OdDHL increases the survival of these
418 cells in the presence of tumor microenvironmental stressors. Finally, although we show that
419 OdDHL decreases breast viability through inhibition of proliferation as well as cell type and
420 culture condition dependent induction of apoptosis and/or necrosis, future work should establish
421 the cell signaling pathways associated with the differential responses to OdDHL. Li et al. linked
422 the selective action of OdDHL on malignant cell lines to STAT3 activity (21). However, further
423 studies into the mechanism of action of OdDHL with our experimental conditions are required to
424 see if this explanation also extends to our data.
425
426 The breast cancer response to OdDHL described above demonstrates that there is significant
427 interaction between bacterial factors and chemical or physical stresses (e.g. hypoxia and stiff
428 ECM) in the tumor microenvironment. Interestingly, in the case of MDA-MB-231 and MCF-
429 DCIS.com cells, we demonstrated that malignant cell hypoxia- and adhesion-mediated resistance
430 are not purely associated with chemotherapeutic compounds, but with native microbiome
431 signaling molecules as well. However, it is also notable that, although the MDA-MB-231 cells

bioRxiv preprint doi: https://doi.org/10.1101/132092; this version posted April 28, 2017. The copyright holder for this preprint (which was not certified by peer review) is the author/funder. All rights reserved. No reuse allowed without permission.

demonstrated a blunted response to OdDHL in hypoxia and in 3D, there was still a significant response. Thus, future studies into both microbiome-tumor interactions and the therapeutic potential of OdDHL could provide valuable information.

Many open questions remain regarding the physiological or pathological role of the breast resident microbiome. Prior research has established an association between the composition of the breast microbiota and cancer, demonstrating the ability of the abundant bacteria in breast cancer patients to induce double-stranded DNA breaks and/or cell proliferation (9). However, it is not yet known whether these microbiome compositions are a cause or consequence of the malignancies (9). Our data provide an important contribution to this field, demonstrating that even for one quorum-sensing molecule there is a complex breast cell response that is dependent on both cell type as well as microenvironmental context. Many more studies of breast relevant bacteria secreted molecules are needed to establish the impact of the soluble factor crosstalk between the microbiome and breast cancer during the entire course of progression as well as during therapy response. With our data, we have established the importance of performing these investigations in the context of physiologically relevant *in vitro* models. Thus, such investigations would benefit from the incorporation of microenvironmental stressors. More broadly, co-culture experiments investigating soluble factor interactions between breast tissue relevant bacteria and cancer cells in the context of tumor microenvironmental stressors could provide valuable insights into carcinogenesis as well as patient-to-patient variability in disease course and therapy response.

bioRxiv preprint doi: https://doi.org/10.1101/132092; this version posted April 28, 2017. The copyright holder for this preprint (which was not certified by peer review) is the author/funder. All rights reserved. No reuse allowed without permission.

454 **Conclusions** We showed that the selective effect of OdDHL on the viability of breast cancer
455 cells is significantly mitigated by two key hallmarks of the tumor microenvironment: hypoxia
456 and stiff ECM. It is important to note that, although there was a blunted response to OdDHL
457 treatment for MDA-MB-231 cells in hypoxia and in 3D, there was still a significant decrease in
458 proliferation and viability, and a significant increase in necrosis with treatment. The intermediary
459 response of MCF-DCIS.com may demonstrate a differential role of microenvironmental bacterial
460 factors over the course of breast cancer progression. Thus, further exploration of microbiome-
461 tumor interactions and OdDHL as a potential therapy is merited.
462
463 **Acknowledgements** We would like to thank Sara Peterson for her assistance in experimental
464 preparation. We would also like to thank Dr. Akanksha Kanitkar for her thoughtful discussions,
465 and Dr. Ann Stevens for useful input on the role of OdDHL in bacterial stress response.
466

bioRxiv preprint doi: https://doi.org/10.1101/132092; this version posted April 28, 2017. The copyright holder for this preprint (which was not certified by peer review) is the author/funder. All rights reserved. No reuse allowed without permission.

Works Cited

1. Shieh AC. Biomechanical forces shape the tumor microenvironment. Annals of biomedical engineering. 2011;39(5):1379-89.

2. Koumoutsakos P, Pivkin I, Milde F. The Fluid Mechanics of Cancer and Its Therapy. Annu Rev Fluid Mech. 2013;45:325-55.

3. Jain RK. Normalizing tumor microenvironment to treat cancer: bench to bedside to biomarkers. Journal of clinical oncology : official journal of the American Society of Clinical Oncology. 2013;31(17):2205-18.

4. Quail DF, Joyce JA. Microenvironmental regulation of tumor progression and metastasis. Nature medicine. 2013;19(11):1423-37.

5. Cummins J, Tangney M. Bacteria and tumours: causative agents or opportunistic inhabitants? Infectious agents and cancer. 2013;8(1):1.

6. Polk DB, Peek RM. Helicobacter pylori: gastric cancer and beyond. Nature Reviews Cancer. 2010;10(6):403-14.

7. Hieken TJ, Chen J, Hoskin TL, Walther-Antonio M, Johnson S, Ramaker S, et al. The Microbiome of Aseptically Collected Human Breast Tissue in Benign and Malignant Disease. Scientific reports. 2016;6:30751.

8. Garrett WS. Cancer and the microbiota. Science. 2015;348(6230):80-6.

9. Urbaniak C, Gloor GB, Brackstone M, Scott L, Tangney M, Reid G. The microbiota of breast tissue and its association with breast cancer. Applied and environmental microbiology. 2016;82(16):5039-48.

10. Xuan C, Shamonki JM, Chung A, DiNome ML, Chung M, Sieling PA, et al. Microbial dysbiosis is associated with human breast cancer. PloS one. 2014;9(1):e83744.

bioRxiv preprint doi: https://doi.org/10.1101/132092; this version posted April 28, 2017. The copyright holder for this preprint (which was not certified by peer review) is the author/funder. All rights reserved. No reuse allowed without permission.

491 11. Reid G. Can breast microbiota provide protective effects against cancer? : Future
492 Medicine; 2016.
493 12. Urbaniak C, Cummins J, Brackstone M, Macklaim JM, Gloor GB, Baban CK, et al.
494 Microbiota of human breast tissue. Applied and environmental microbiology. 2014;80(10):3007-
495 14.
496 13. Chan AA, Bashir M, Rivas MN, Duvall K, Sieling PA, Pieber TR, et al. Characterization
497 of the microbiome of nipple aspirate fluid of breast cancer survivors. Scientific reports.
498 2016;6:28061.
499 14. McGuire MK, McGuire MA. Got bacteria? The astounding, yet not-so-surprising,
500 microbiome of human milk. Current Opinion in Biotechnology. 2017;44:63-8.
501 15. Gomez-Gallego C, Garcia-Mantrana I, Salminen S, Collado MC. The human milk
502 microbiome and factors influencing its composition and activity. Seminars in Fetal and Neonatal
503 Medicine. 2016;21(6):400-5.
504 16. Hoashi M, Meche L, Mahal LK, Bakacs E, Nardella D, Naftolin F, et al. Human Milk
505 Bacterial and Glycosylation Patterns Differ by Delivery Mode. Reproductive Sciences.
506 2015;23(7):902-7.
507 17. García-Contreras R, Nunez-Lopez L, Jasso-Chávez R, Kwan BW, Belmont JA, Rangel-
508 Vega A, et al. Quorum sensing enhancement of the stress response promotes resistance to
509 quorum quenching and prevents social cheating. The ISME journal. 2015;9(1):115-25.
510 18. Tao S, Luo Y, He B, Liu J, Qian X, Ni Y, et al. Paraoxonase 2 modulates a proapoptotic
511 function in LS174T cells in response to quorum sensing molecule N-(3-oxododecanoyl)-L-
512 homoserine lactone. Scientific reports. 2016;6.

bioRxiv preprint doi: https://doi.org/10.1101/132092; this version posted April 28, 2017. The copyright holder for this preprint (which was not certified by peer review) is the author/funder. All rights reserved. No reuse allowed without permission.

513 19. Schwarzer C, Fu Z, Patanwala M, Hum L, Lopez-Guzman M, Illek B, et al. Pseudomonas
514 aeruginosa biofilm-associated homoserine lactone C12 rapidly activates apoptosis in airway
515 epithelia. Cellular microbiology. 2012;14(5):698-709.
516 20. Tateda K, Ishii Y, Horikawa M, Matsumoto T, Miyairi S, Pechere JC, et al. The
517 Pseudomonas aeruginosa Autoinducer N-3-Oxododecanoyl Homoserine Lactone Accelerates
518 Apoptosis in Macrophages and Neutrophils. Infection and Immunity. 2003;71(10):5785-93.
519 21. Li L, Hooi D, Chhabra SR, Pritchard D, Shaw PE. Bacterial N-acylhomoserine lactone-
520 induced apoptosis in breast carcinoma cells correlated with down-modulation of STAT3.
521 Oncogene. 2004;23(28):4894-902.
522 22. Shiner E, Terentyev D, Bryan A, Sennoune S, Martinez□Zaguilan R, Li G, et al.
523 Pseudomonas aeruginosa autoinducer modulates host cell responses through calcium signalling.
524 Cellular microbiology. 2006;8(10):1601-10.
525 23. Jacobi CA, Schiffner F, Henkel M, Waibel M, Stork B, Daubrawa M, et al. Effects of
526 bacterial N-acyl homoserine lactones on human Jurkat T lymphocytes-OdDHL induces apoptosis
527 via the mitochondrial pathway. International Journal of Medical Microbiology. 2009;299(7):509-
528 19.
529 24. Kumar AS, Bryan JN, Kumar SR. Bacterial quorum sensing molecule N-3-oxo-
530 dodecanoyl-L-homoserine lactone causes direct cytotoxicity and reduced cell motility in human
531 pancreatic carcinoma cells. PloS one. 2014;9(9):e106480.
532 25. Zhao G, Neely AM, Schwarzer C, Lu H, Whitt AG, Stivers NS, et al. N-(3-oxo-acyl)
533 homoserine lactone inhibits tumor growth independent of Bcl-2 proteins. Oncotarget.
534 2016;7(5):5924-42.

bioRxiv preprint doi: https://doi.org/10.1101/132092; this version posted April 28, 2017. The copyright holder for this preprint (which was not certified by peer review) is the author/funder. All rights reserved. No reuse allowed without permission.

535 26. Checka CM, Chun JE, Schnabel FR, Lee J, Toth H. The relationship of mammographic
536 density and age: implications for breast cancer screening. American Journal of Roentgenology.
537 2012;198(3):W292-W5.
538 27. Infanger DW, Lynch ME, Fischbach C. Engineered culture models for studies of tumor-
539 microenvironment interactions. Annual review of biomedical engineering. 2013;15:29-53.
540 28. Pelham RJ, Wang Y-l. Cell locomotion and focal adhesions are regulated by substrate
541 flexibility. Proceedings of the National Academy of Sciences. 1997;94(25):13661-5.
542 29. Edmondson R, Broglie JJ, Adcock AF, Yang L. Three-dimensional cell culture systems
543 and their applications in drug discovery and cell-based biosensors. Assay and drug development
544 technologies. 2014;12(4):207-18.
545 30. DelNero P, Lane M, Verbridge SS, Kwee B, Kermani P, Hempstead B, et al. 3D culture
546 broadly regulates tumor cell hypoxia response and angiogenesis via pro-inflammatory pathways.
547 Biomaterials. 2015;55:110-8.
548 31. Seguin L, Desgrosellier JS, Weis SM, Cheresh DA. Integrins and cancer: regulators of
549 cancer stemness, metastasis, and drug resistance. Trends in cell biology. 2015;25(4):234-40.
550 32. Eke I, Cordes N, editors. Focal adhesion signaling and therapy resistance in cancer.
551 Seminars in cancer biology; 2015: Elsevier.
552 33. Ward C, Langdon SP, Mullen P, Harris AL, Harrison DJ, Supuran CT, et al. New
553 strategies for targeting the hypoxic tumour microenvironment in breast cancer. Cancer treatment
554 reviews. 2013;39(2):171-9.
555 34. Rohwer N, Cramer T. Hypoxia-mediated drug resistance: novel insights on the functional
556 interaction of HIFs and cell death pathways. Drug Resistance Updates. 2011;14(3):191-201.

bioRxiv preprint doi: https://doi.org/10.1101/132092; this version posted April 28, 2017. The copyright holder for this preprint (which was not certified by peer review) is the author/funder. All rights reserved. No reuse allowed without permission.

557 35. Chavez KJ, Garimella SV, Lipkowitz S. Triple Negative Breast Cancer Cell Lines: One
558 Tool in the Search for Better Treatment of Triple Negative Breast Cancer. Breast disease.
559 2010;32(1-2):35-48.
560 36. Cowell JK, LaDuca J, Rossi MR, Burkhardt T, Nowak NJ, Matsui S-i. Molecular
561 characterization of the t(3;9) associated with immortalization in the MCF10A cell line. Cancer
562 Genetics and Cytogenetics. 2005;163(1):23-9.
563 37. So JY, Lee HJ, Kramata P, Minden A, Suh N. Differential Expression of Key Signaling
564 Proteins in MCF10 Cell Lines, a Human Breast Cancer Progression Model. Molecular and
565 cellular pharmacology. 2012;4(1):31-40.
566 38. Miller FR, Santner SJ, Tait L, Dawson PJ. MCF10DCIS. com xenograft model of human
567 comedo ductal carcinoma in situ. Journal of the National Cancer Institute. 2000;92(14):1185a-6.
568 39. Yen T-H, Lee G-D, Chai J-W, Liao J-W, Lau J-Y, Hu L-C, et al. Characterization of a
569 murine xenograft model for contrast agent development in breast lesion malignancy assessment.
570 Journal of Biomedical Science. 2016;23(1):46.
571 40. Nelson MT, Short A, Cole SL, Gross AC, Winter J, Eubank TD, et al. Preferential,
572 enhanced breast cancer cell migration on biomimetic electrospun nanofiber 'cell highways'.
573 BMC cancer. 2014;14(1):825.
574 41. Cross VL, Zheng Y, Choi NW, Verbridge SS, Sutermaster BA, Bonassar LJ, et al. Dense
575 type I collagen matrices that support cellular remodeling and microfabrication for studies of
576 tumor angiogenesis and vasculogenesis in vitro. Biomaterials. 2010;31(33):8596-607.
577 42. Lazenby JJ. The role of N-(3-oxododecanoyl)-L-homoserine lactone in the pathogenesis
578 of Pseudomonas aeruginosa [Ph.D.]: University of New South Wales; 2011.

bioRxiv preprint doi: https://doi.org/10.1101/132092; this version posted April 28, 2017. The copyright holder for this preprint (which was not certified by peer review) is the author/funder. All rights reserved. No reuse allowed without permission.

579 43. Dolnick R, Wu Q, Angelino NJ, Stephanie LV, Chow K-C, Sufrin JR, et al. Enhancement
580 of 5-Fluorouracil Sensitivity by an rTS Signaling Mimic in H630 Colon Cancer Cells. Cancer
581 Research. 2005;65(13):5917-24.
582 44. Proskuryakov SYa, Konoplyannikov AG, Gabai VL. Necrosis: a specific form of
583 programmed cell death? Experimental Cell Research. 2003;283(1):1-16.
584

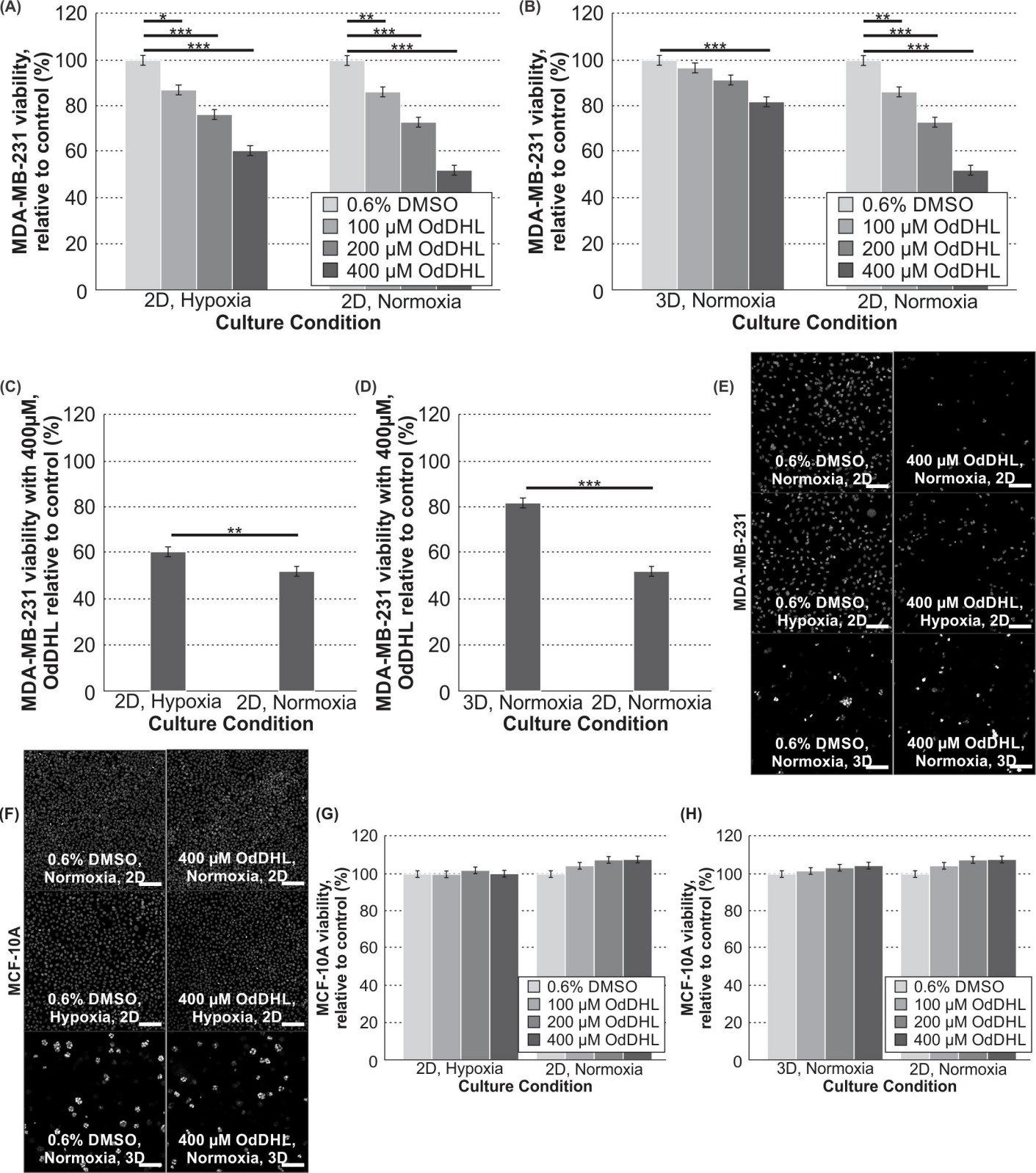
(A)
MDA-MB-231 viability, relative to control (%)
120
100
80
60
40
20
0
*
***
***
**
***
***
0.6% DMSO
100 μM OdDHL
200 μM OdDHL
400 μM OdDHL
2D, Hypoxia
2D, Normoxia
Culture Condition
(B)
MDA-MB-231 viability, relative to control (%)
***
**
***
***
0.6% DMSO
100 μM OdDHL
200 μM OdDHL
400 μM OdDHL
3D, Normoxia
2D, Normoxia
Culture Condition
(C)
MDA-MB-231 viability with 400μM, OdDHL relative to control (%)
**
2D, Hypoxia
2D, Normoxia
Culture Condition
(D)
MDA-MB-231 viability with 400μM, OdDHL relative to control (%)
***
3D, Normoxia
2D, Normoxia
Culture Condition
(E)
MDA-MB-231
0.6% DMSO, Normoxia, 2D
400 μM OdDHL, Normoxia, 2D
0.6% DMSO, Hypoxia, 2D
400 μM OdDHL, Hypoxia, 2D
0.6% DMSO, Normoxia, 3D
400 μM OdDHL, Normoxia, 3D
(F)
MCF-10A
0.6% DMSO, Normoxia, 2D
400 μM OdDHL, Normoxia, 2D
0.6% DMSO, Hypoxia, 2D
400 μM OdDHL, Hypoxia, 2D
0.6% DMSO, Normoxia, 3D
400 μM OdDHL, Normoxia, 3D
(G)
MCF-10A viability, relative to control (%)
0.6% DMSO
100 μM OdDHL
200 μM OdDHL
400 μM OdDHL
2D, Hypoxia
2D, Normoxia
Culture Condition
(H)
MCF-10A viability, relative to control (%)
0.6% DMSO
100 μM OdDHL
200 μM OdDHL
400 μM OdDHL
3D, Normoxia
2D, Normoxia
Culture Condition

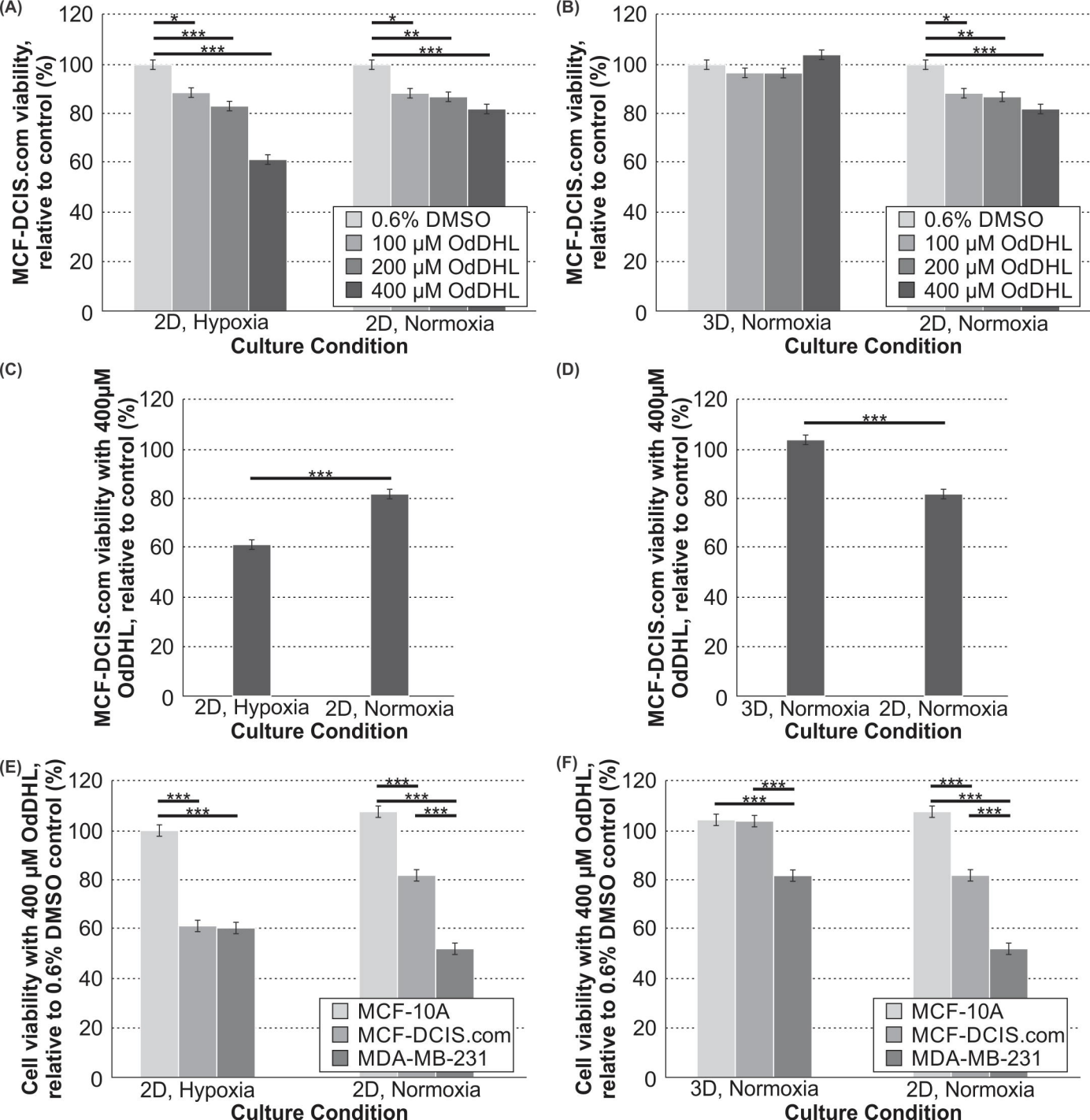
(A)
MCF-DCIS.com viability, relative to control (%)
0.6% DMSO
100 μM OdDHL
200 μM OdDHL
400 μM OdDHL
2D, Hypoxia
2D, Normoxia
Culture Condition
(B)
MCF-DCIS.com viability, relative to control (%)
3D, Normoxia
2D, Normoxia
Culture Condition
(C)
MCF-DCIS.com viability with 400μM OdDHL, relative to control (%)
2D, Hypoxia
2D, Normoxia
Culture Condition
(D)
MCF-DCIS.com viability with 400μM OdDHL, relative to control (%)
3D, Normoxia
2D, Normoxia
Culture Condition
(E)
Cell viability with 400 μM OdDHL, relative to 0.6% DMSO control (%)
MCF-10A
MCF-DCIS.com
MDA-MB-231
2D, Hypoxia
2D, Normoxia
Culture Condition
(F)
Cell viability with 400 μM OdDHL, relative to 0.6% DMSO control (%)
MCF-10A
MCF-DCIS.com
MDA-MB-231
3D, Normoxia
2D, Normoxia
Culture Condition

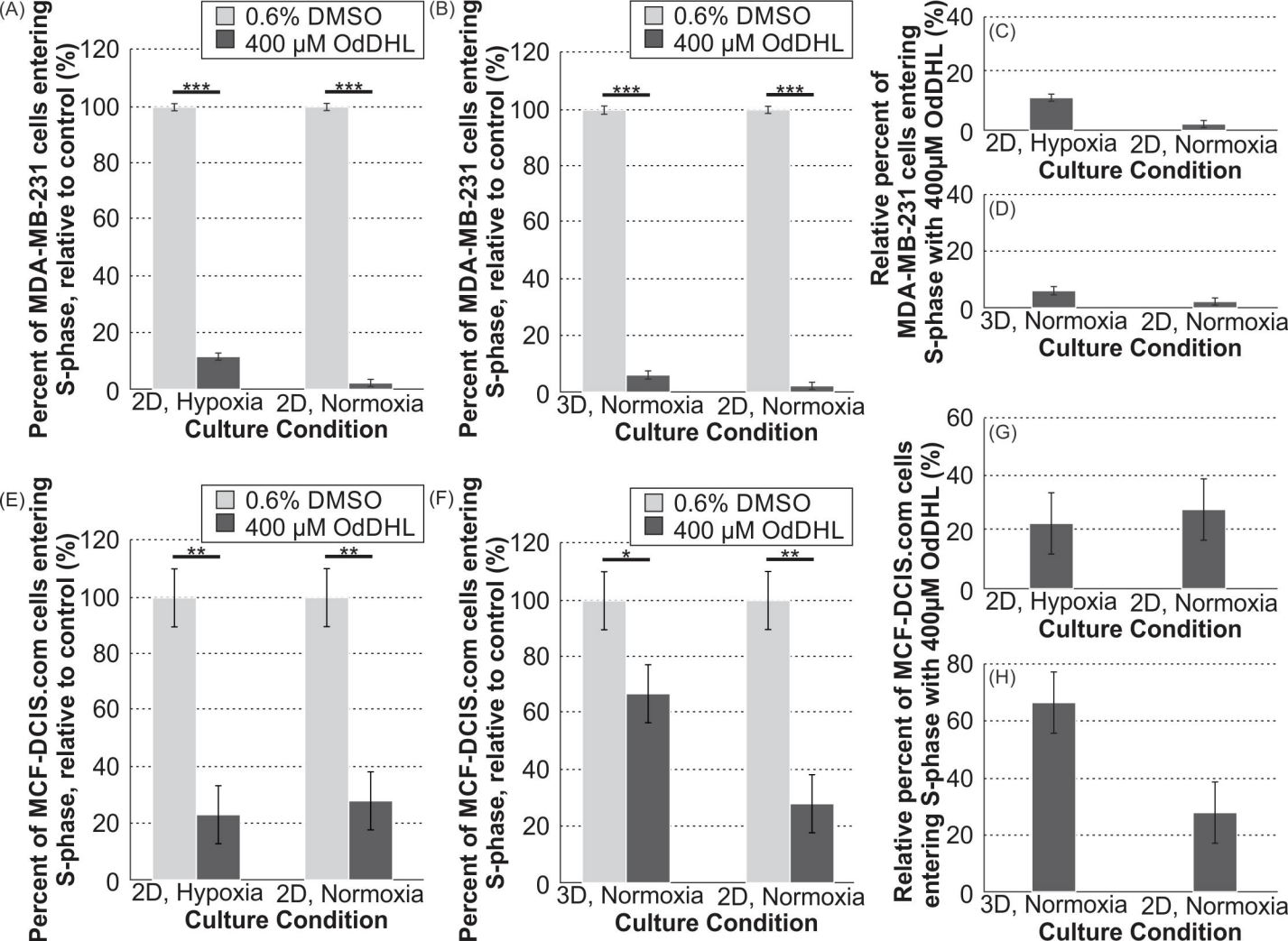
(A)
0.6% DMSO
400 μM OdDHL
Percent of MDA-MB-231 cells entering S-phase, relative to control (%)
120
100
80
60
40
20
0
***
***
2D, Hypoxia
2D, Normoxia
Culture Condition
(B)
0.6% DMSO
400 μM OdDHL
Percent of MDA-MB-231 cells entering S-phase, relative to control (%)
***
***
3D, Normoxia
2D, Normoxia
Culture Condition
(C)
Relative percent of MDA-MB-231 cells entering S-phase with 400μM OdDHL (%)
40
20
0
2D, Hypoxia
2D, Normoxia
Culture Condition
(D)
40
20
0
3D, Normoxia
2D, Normoxia
Culture Condition
(E)
0.6% DMSO
400 μM OdDHL
Percent of MCF-DCIS.com cells entering S-phase, relative to control (%)
120
100
80
60
40
20
0
**
**
2D, Hypoxia
2D, Normoxia
Culture Condition
(F)
0.6% DMSO
400 μM OdDHL
Percent of MCF-DCIS.com cells entering S-phase, relative to control (%)
*
**
3D, Normoxia
2D, Normoxia
Culture Condition
(G)
Relative percent of MCF-DCIS.com cells entering S-phase with 400μM OdDHL (%)
60
40
20
0
2D, Hypoxia
2D, Normoxia
Culture Condition
(H)
80
60
40
20
0
3D, Normoxia
2D, Normoxia
Culture Condition

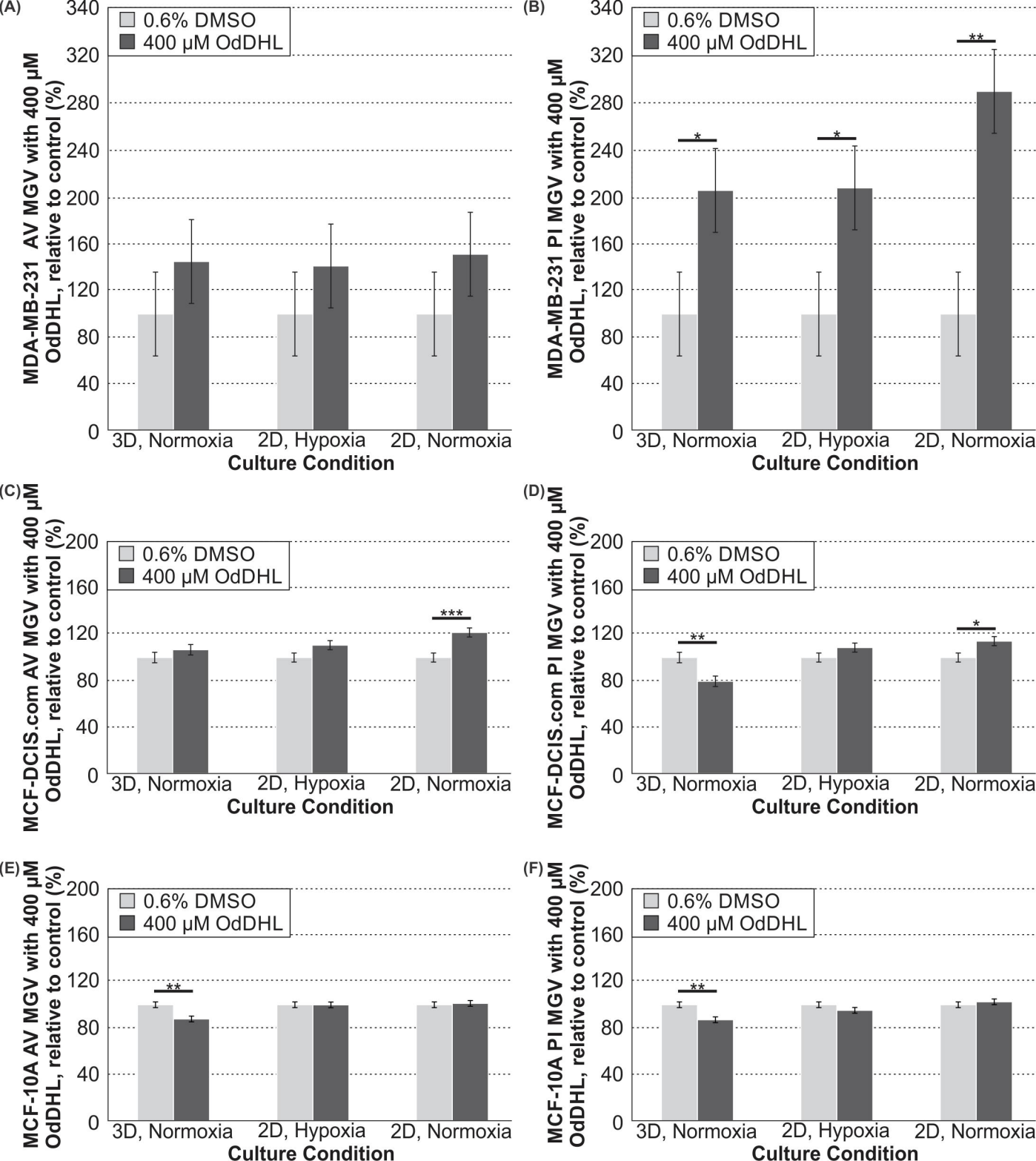
(A)
MDA-MB-231 AV MGV with 400 µM OdDHL, relative to control (%)
0.6% DMSO
400 µM OdDHL
3D, Normoxia
2D, Hypoxia
2D, Normoxia
Culture Condition
(B)
MDA-MB-231 PI MGV with 400 µM OdDHL, relative to control (%)
*
*
**
(C)
MCF-DCIS.com AV MGV with 400 µM OdDHL, relative to control (%)
***
(D)
MCF-DCIS.com PI MGV with 400 µM OdDHL, relative to control (%)
**
*
(E)
MCF-10A AV MGV with 400 µM OdDHL, relative to control (%)
**
(F)
MCF-10A PI MGV with 400 µM OdDHL, relative to control (%)
**